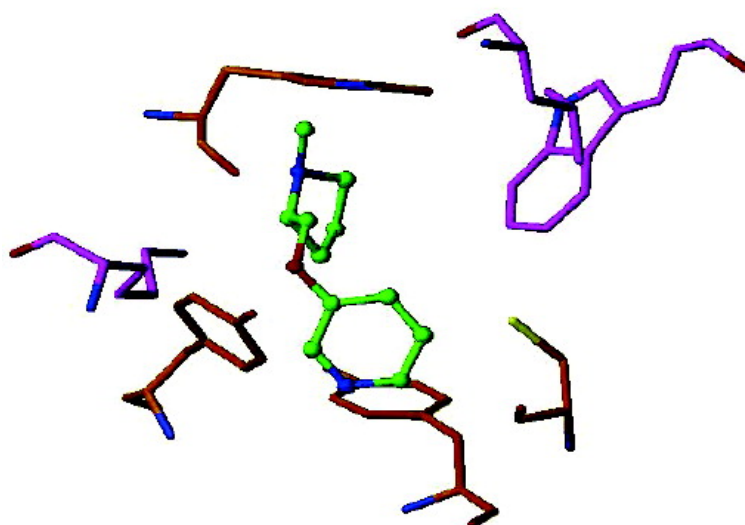


## Ligand Selectivity for the Acetylcholine Binding Site of the Rat $\alpha 4\beta 2$ and $\alpha 3\beta 4$ Nicotinic Subtypes Investigated by Molecular Docking

William H. Bisson, Leonardo Scapozza, Gerrit Westera, Linjing Mu, and P. A. Schubiger

*J. Med. Chem.*, 2005, 48 (16), 5123-5130 • DOI: 10.1021/jm040881a • Publication Date (Web): 14 July 2005

Downloaded from <http://pubs.acs.org> on March 28, 2009



### More About This Article

Additional resources and features associated with this article are available within the HTML version:

- Supporting Information
- Links to the 1 articles that cite this article, as of the time of this article download
- Access to high resolution figures
- Links to articles and content related to this article
- Copyright permission to reproduce figures and/or text from this article

[View the Full Text HTML](#)

# Ligand Selectivity for the Acetylcholine Binding Site of the Rat $\alpha 4\beta 2$ and $\alpha 3\beta 4$ Nicotinic Subtypes Investigated by Molecular Docking

William H. Bisson,<sup>‡</sup> Leonardo Scapozza,<sup>§</sup> Gerrit Westera,<sup>\*,‡</sup> Linjing Mu,<sup>‡</sup> and P. A. Schubiger<sup>‡</sup>

Center for Radiopharmaceutical Sciences, Swiss Federal Institute of Technology Zurich, Paul Scherrer Institute, Villigen and University Hospital of Zürich, Rämistrasse 100, CH-8091 Zürich, Switzerland, and Pharmaceutical Biochemistry, Institute of Pharmaceutical Sciences, Swiss Federal Institute of Technology Zürich, Hönggerberg, Wolfgang Pauli strasse 10, CH-8093 Zürich, Switzerland

Received September 27, 2004

The homology models of the extracellular domains of the neuronal  $\alpha 4\beta 2$  (pdb code: 1ole) and ganglionic  $\alpha 3\beta 4$  (pdb code: 1olf) rat nicotinic acetylcholine receptor (nAChR) subtypes were refined and energetically minimized. In this work, a series of nAChR ligands (**1–15**) were docked into the modeled binding cavity of both receptors. High-affinity, toxic ligands such as epibatidine (**1**) and dechloroepibatidine (**2**) docked into cluster 1 with the charged tertiary amino group, forming a  $\pi$ -cation interaction with Trp 147 on the (+) side of the  $\alpha 4$  subunit and establishing a characteristic H-bond with the Lys 77 on the (–) side of the  $\beta 2$  subunit. The nontoxic ligands such as 33bMet (**3**), (S)-A-85380 (**4**), and acetylcholine (**6**) docked into cluster 2 with the same  $\pi$ -cation interaction but with the rest of the molecule occupying a different moiety of the binding pocket. Molecular docking into the  $\alpha 3\beta 4$  subtype showed that both enantiomers of **1** (**1a** and **1b**) are representative templates for ligands with affinity toward this ganglionic nAChR subtype. The ranking scores of the docked molecules confirm the existence of structure-dependent subtype selectivity and shed light on the design of specific and selective  $\alpha 4\beta 2$  nAChR subtype ligands.

## Introduction

The nicotinic acetylcholine receptor (nAChR) is a member of the “cys-loop” superfamily of ligand-gated ion channels, which also comprises GABA<sub>A</sub>C, glycine, and 5-HT<sub>3</sub> receptors.<sup>1,2</sup> In the central nervous system, neuronal nAChRs are located post- and presynaptically or even on axonic areas of the neuron.<sup>3</sup> They mediate acetylcholine (**6**) neurotransmission<sup>4</sup> at the neuromuscular junction, the autonomic ganglia, and the central nervous system. nAChRs are composed of five polypeptide chains (subunits). They may be identical (homopentamers) or different (heteropentamers). These subunits, which form a cation-permeable pore around an axis that is perpendicular to the membrane, build different subtypes. The binding sites are located at the interface between two extracellular subunits, and their number differs according to the subtype. As a consequence, in vertebrates, the assembly of  $\alpha 1-10$ ,  $\beta 1-4$ ,  $\gamma$ ,  $\delta$ , and  $\epsilon$  subunits allows for a variety of receptors with different electrical and binding characteristics.<sup>5</sup> The existing different neuronal nAChR subtypes can be stimulated by epibatidine (**1**),<sup>6</sup> by nicotine (**7**), or by synthetic compounds.<sup>7,8</sup> Recently, it has been demonstrated that neuronal nAChRs, because of their important physiological and pharmacological role, may be a useful therapeutic target in a variety of diseases, including Alzheimer's, anxiety, and nicotine addiction.<sup>5,9</sup> Thus, the development of brain-specific nAChR ligands is a worthwhile goal. Subtype selectivity is still an elusive problem. Compound **1** has one of the highest binding affinities for the neuronal  $\alpha 4\beta 2$  subtype. On the other

hand, it shows potent agonist activity for sympathetic receptors such as the ganglionic ( $\alpha 3$ -containing) and neuromuscular ( $\alpha 1\beta 1\gamma\delta$ ) nAChR subtypes.<sup>10,11</sup> The activity of **1** at the peripheral nAChRs is probably responsible for the hypertension and muscular paralysis<sup>11</sup> observed after in vivo application. Hence, the use of **1** results in a very limited therapeutic index that has precluded its clinical usefulness as an analgesic. In vivo applications have indicated that many toxic clinical side effects originate from the lack of selectivity of ligands toward specific subtype receptors. To address the selectivity issue of the nAChR ligand, the newly available structural information of the acetylcholine-binding protein (AChBP) may be used.

The crystal structure of AChBP has recently been determined.<sup>12</sup> It is a soluble homopentamer that is produced and stored in glial cells and is released into the synaptic cleft to modulate synaptic transmission.<sup>13</sup> AChBP binds nAChR agonists and competitive antagonists such as **6**, **7**, *d*-tubocurarine, and  $\alpha$ -bungarotoxin.<sup>13</sup> The sequence identity between AChBP and  $\alpha$  and  $\beta$  nAChR subunits is significant (23–26%). Therefore, AChBP can be exploited as a template of the N-terminal domain (which comprises the binding site) of the  $\alpha$  and  $\beta$  subunits of nAChRs. The homology models of the extracellular domains of the neuronal rat ( $\alpha 4$ )<sub>2</sub>( $\beta 2$ )<sub>3</sub> and the ganglionic rat ( $\alpha 3$ )<sub>2</sub>( $\beta 4$ )<sub>3</sub> nAChR subtypes can now be downloaded from the Protein Data Bank.

In the present work, we used the refined and energetically minimized binding site of both models to perform molecular docking. A series of nAChR ligands (**1–15**) have been docked into the binding cavities to investigate their selectivity toward the neuronal and the ganglionic nAChR subtypes.

\* To whom correspondence should be addressed. Phone: 41-1-2553560. Fax: 41-1-2554428. E-mail: gerrit.westera@usz.ch.

<sup>‡</sup> Center for Radiopharmaceutical Sciences.

<sup>§</sup> Institute of Pharmaceutical Sciences.

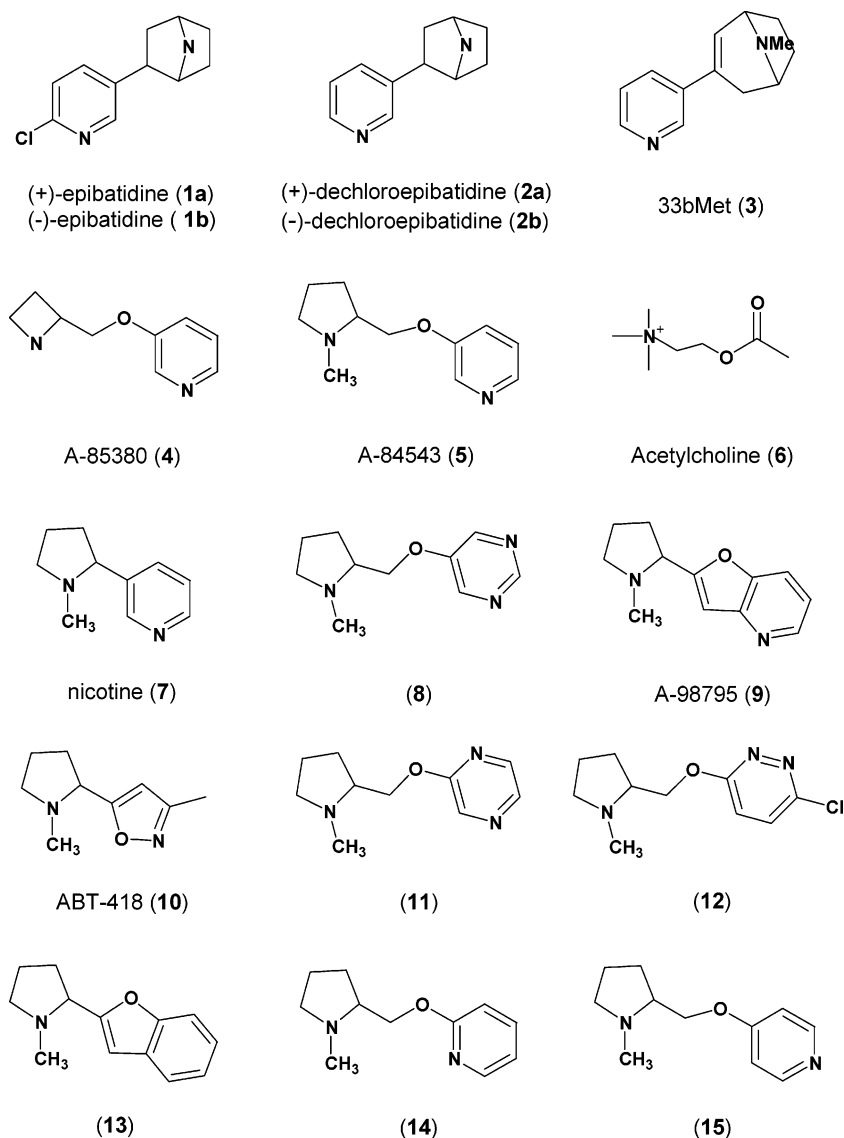


**Figure 1.** Nicotinic ligands docked into the  $(\alpha 4)_2(\beta 2)_3$  and  $(\alpha 3)_2(\beta 4)_3$  binding sites. Both enantiomers of compound **3** were docked. Compounds **4**, **5**, and **7–15** were docked in their *S*-enantiomeric form.

## Material and Methods

**Preparation of the Three-Dimensional (3D) Targets.** Starting from the downloaded 3D templates snail AChBP (pdb code: 1i9b) and rat  $\alpha 4\beta 2$  (pdb code: 1ole) and  $\alpha 3\beta 4$  (pdb code: 1olf) pentamers, the 3D models were refined, geometrically improved with the software SYBYL 6.8 provided by Tripos Inc. (St. Louis, USA), and minimized via the program AMBER6 (Assisted Model Building with Energy Refinement) provided by the University of California (USA). The models were initially boxed with water molecules; counterions ( $\text{Na}^+$ ) were then added to get charge neutrality, and finally, the models were minimized using the program AMBER6.

The AMBER force field<sup>14</sup> all-atom parameters (parm94) were used for the protein and the  $\text{Na}^+$  ions. Periodic boundary conditions were applied. The minimization protocol consisted of 1000 cycles of steepest descent followed by the conjugate gradient method. The primary cutoff distance for nonbonded interaction was set at 9 Å. During the different steps, the stereochemical quality of the model was assessed using the program PROCHECK.<sup>15</sup>

**Preparation of the 3D Database of the Ligands and Molecular Docking.** The nAChR ligands (**1–15**) (Figure 1) to be docked were selected ranging in affinity values for the rat  $\alpha 4\beta 2$  nAChR subtype from picomolar to micromolar<sup>16,17</sup> (Table 1). The 3D structure of the compounds was built with the program SYBYL 6.8. Hydrogen atoms were added, and Gasteiger atomic charges were calculated. Ligands were calculated and energetically minimized in their neutral and positively charged form. The final coordinates of each compound were saved as a mol2 file, and all files were then stored in a single database. The docking of all nicotinic ligands on both subtype models was performed via the program FlexX<sup>18,19</sup> implemented in SYBYL 6.8, which used flexibility positioning for the ligands to be placed into the active site on the basis of the principles of shape and electrostatic and hydrophobic/polar complementarity.<sup>19</sup> A time calculation of ~3 min per compound was required to dock the ligand in the flexible mode. For each ligand, the 10 energetically most favorable docking orientations were calculated. The consensus scoring program CScore<sup>20</sup> integrates five individual scoring functions (DOCK-like, ChemScore, PMF, GOLD-like,

**Table 1.** Docking, Affinity, and Toxicity Data of All Ligands Investigated<sup>a</sup>

	CScore $\alpha 4\beta 2$	cluster $\alpha 4\beta 2$	CScore $\alpha 3\beta 4$	$K_i$ (nM) <sup>b</sup> $\alpha 4\beta 2$	$K_i$ (nM) <sup>c</sup> $\alpha 3\beta 4$	EC50 ( $\mu$ M) $\alpha 3\beta 4$	LD50 <sup>d</sup> (nmol/kg)	ref
<b>1a</b>	5	1	3	0.05	0.38 <sup>e</sup>	0.7 <sup>e,f</sup>	7–67	31–34
<b>1b</b>	5	1	3	0.073	0.38 <sup>e</sup>	0.7 <sup>e,f</sup>	7–67	31–34
<b>2a</b>	5	1	5	0.064 <sup>g</sup>	nd	0.51 <sup>h</sup>	12–120	26
<b>2b</b>	5	1	3	0.015 <sup>g,i</sup>	nd	0.25 <sup>h</sup>	12–120	26
<b>3<sup>j</sup></b>	5	2	5	2.07	nd	nd	250	<i>k</i>
<b>4</b>	4	2	0	0.05	73.6	nd	1200–10 <sup>4</sup>	16, 32, 34
<b>5</b>	3	3	0	0.15		63 <sup>f</sup>	1200–10 <sup>4</sup>	17, 33, 34
<b>6</b>	2	2	0 <sup>l</sup>	7.6 <sup>m</sup>	881		1.38 $\times$ 10 <sup>7</sup>	32, 35, 36
<b>8</b>	0	4	0	2.39	nd	nd	nd	17
<b>9</b>	nd		5	2.7	nd	<i>k</i>	nd	16
<b>10</b>	3	3	0	4		209 <sup>n</sup>	1.37 $\times$ 10 <sup>5</sup>	16, 37
<b>11</b>	0	4	0	16.3	nd	nd	nd	17
<b>12</b>	1	4	0	29	nd	nd	nd	17
<b>13</b>	nd	5	158	nd	nd	nd	nd	16
<b>14</b>	2	3	0	495	nd	nd	nd	17
<b>15</b>	2	3	0	7914	nd	nd	nd	17

<sup>a</sup> nd = not determined. <sup>b</sup> Displacement studies with [<sup>3</sup>H]cytisine on brain homogenates. <sup>c</sup> Displacement studies with [<sup>3</sup>H]epibatidine on heterologously expressed nAChRs. <sup>d</sup> Performed in rodents. <sup>e</sup> ( $\pm$ )-epibatidine data. <sup>f</sup> Functional potencies reported for heterologously expressed nAChRs on an IMR32 cell. <sup>g</sup> Brain homogenates without cerebellum. <sup>h</sup> Functional potencies reported for heterologously expressed nAChRs on *Xenopus* oocytes. <sup>i</sup> IC<sub>50</sub> data. <sup>j</sup> Same results for both enantiomers. <sup>k</sup> Unpublished data. <sup>l</sup> Ligand does not dock deeply into the binding cavity. <sup>m</sup> Displacement binding studies with [<sup>3</sup>H]acetylcholine on brain homogenates. <sup>n</sup> Functional potencies reported for heterologously expressed nAChRs on PC12 cells.

and FlexX) to predict the affinity of the ligands in candidate complexes. The DOCK-like function considers electrostatic and hydrophobic contributions; the ChemScore estimates lipophilic interactions, H-bonding, and loss of ligand flexibility; the PMF function is based upon ligand–receptor atom-pair interaction potentials (solvation and entropic terms are treated); the GOLD-like function focuses on H-bond interactions; and the FlexX scoring function accounts for H-bonds, salt bridges, and nonpolar interaction distances. Entropic and enthalpic terms are added too.

Each ligand–receptor complex with a score that exceeds the threshold for a particular function adds one to the value of the consensus, whereas scores below the threshold contribute zero. The consensus score for each complex goes from a minimum of 0 to a maximum of 5. Screened compounds and their proposed binding orientation were then ranked on the basis of CScore,<sup>20</sup> which allowed for a more robust evaluation of ligand–receptor interactions than any single function.<sup>21</sup> The reliability of the suggested binding orientation was assessed via CScore.

## Results and Discussion

**Molecular Modeling and Docking.** The 3D structure of the snail AChBP pentamer and the neuronal rat ( $\alpha 4$ )<sub>2</sub>( $\beta 2$ )<sub>3</sub> and ganglionic rat ( $\alpha 3$ )<sub>2</sub>( $\beta 4$ )<sub>3</sub> nAChR subtypes were retrieved from the Protein Data Bank. The three models were refined and geometrically improved relative to the starting templates. The number of cis-configurations of nonproline amino acids and D-chiralities in ( $\alpha 3$ )<sub>2</sub>( $\beta 4$ )<sub>3</sub> was eliminated, and the number of bad contacts was significantly reduced. Thereafter, the models were water boxed, counterions were added to get charge neutrality, and the models were energetically minimized. The quality of the Ramachandran plot of both the refined and the starting ( $\alpha 3$ )<sub>2</sub>( $\beta 4$ )<sub>3</sub> model obtained by PROCHECK<sup>15</sup> reveals an improvement, compared to the starting template, in the percentage of residues found in the disallowed region (from 5.1 to 4.5%).

The inspection of the binding site of the rat ( $\alpha 4$ )<sub>2</sub>( $\beta 2$ )<sub>3</sub> and ( $\alpha 3$ )<sub>2</sub>( $\beta 4$ )<sub>3</sub> pentameric receptors, at the interface

between the adjacent  $\alpha$  and  $\beta$  subunits, revealed high structural similarity with the starting AChBP template.<sup>12</sup> In both models, the (+) and the (–) sides were formed by the  $\alpha$  (different loops) subunit and the  $\beta$  (a series of  $\beta$ -strands) subunit, respectively. Together the two subunits form the binding-site cleft. The homology at the residue level involved mostly the (+) side, whereas the residues forming the (–) side were less conserved. This homology is also conserved at the 3D level, especially in the binding-site region between the two adjacent subunits.<sup>22</sup> This suggests that the ligand may bind and have different interactions according to the subtype involved, especially at the  $\beta$  subunit region.

To validate the protocol, the docking was initially applied to the X-ray structure of AChBP.<sup>12</sup> The AChBP binding site, containing the buffer molecule *N*-2-hydroxyethylpiperazine-*N'*-2-ethanesulfonic acid (HEPES), is located at the interface between two adjacent monomers that behave, according to their residues, as the (+) and the (–) sides of the binding-site region.<sup>12</sup> HEPES docked into the empty (after the removal of HEPES) binding site of AChBP with a higher consensus score of 5 and with the same orientation found in the X-ray structure (RMSD of all atoms was 1.2 Å). Compound **6**, the natural ligand of AChBP, also docked with a higher consensus score of 5. Figure 2 compares the orientation of HEPES from the X-ray structure and the docked **6** at the AChBP site. HEPES contains a positively charged quaternary ammonium group and stacks with it onto Trp 143, making cation– $\pi$  interactions.<sup>12</sup> The oxygen carbonyl of **6** establishes an H-bond with the O–H of Tyr 192 of the (+) side, whereas the positively charged nitrogen is stabilized, as with HEPES, by cation– $\pi$  noncovalent interactions with the aromatic pocket made of residues Trp 143 and Tyr 185, 192 of the (+) side and Trp 53 of the (–) side of the protein binding site. These data confirm the prediction of the role of  $\alpha$  Tyr 192 in binding the ACh ester group.<sup>23</sup> Residue Trp 143 is believed to be critical for the establishment of cation– $\pi$  interactions with the cationic center of the ligand, which occurs with **7**.<sup>24</sup> The interaction of the ligand with Trp 143 and the assembly of Tyr in the binding cavity are strictly related to the affinity

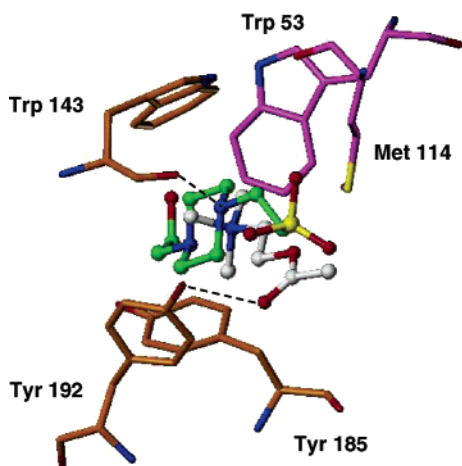


**Figure 2.** Binding site region of the AChBP. Docked **6** is colored according to atom type, with the carbon atoms shown in white; the HEPES from the AChBP crystal structure is colored according to atom type, with the carbon atoms shown in green and the sulfur atom shown in yellow. Residues on the (+) and (−) sides are colored according to atom type with the carbon atoms in orange and magenta, respectively. All residues are displayed as capped sticks, and docked **6** and HEPES are displayed in ball-and-stick format. H-bonds are represented by black dashed lines between the donor (D) and the acceptor (A) and are defined as follows: Distance D⋯A: 2.8–3.2 Å; Angle D–H⋯A: 140–180°.

of the ligand toward the receptor.<sup>25</sup> This shows that the docking protocol used is indeed able to reproduce the characteristic nAChR–ligand interaction.

A series of nAChR ligands (**1–15**) (Figure 1), with binding affinities ranging from picomolar to micromolar, which were determined with displacement binding studies with [<sup>3</sup>H]-cytisine, were chosen to cover a broad range of binding affinity to the rat  $\alpha 4\beta 2$  neuronal nicotinic receptor (Table 1). The selection includes the natural ligand **6**; ligands from natural sources such as **1**; synthetic ligands such as the S-enantiomers A-85380 (**4**), A-84543 (**5**), and ABT-418 (**10**);<sup>16,17</sup> the epibatidine derivative dechloroepibatidine (**2**);<sup>26</sup> and 33bMet (**3**), which was synthesized in our group (Westera, G., unpublished observation).

The group of ligands were initially docked into the binding site of rat  $\alpha 4\beta 2$ , at the interface between the  $\alpha 4$  and  $\beta 2$  subunits, as positive cations and neutral molecules using the validated protocol. The neutral molecules did not dock into the binding site. In contrast, the ligands, in their positively charged form, were docked within the binding site, and the consensus scores were calculated for each docked compound (Table 1). This shows the importance of a positively charged nitrogen in the structure as a pharmacophoric group, which is in agreement with previous pharmacophore analyses.

Two main clusters of binding orientations were identified. Cluster 1 involves residues Trp 147 of the (+) side, Lys 77, Val 109, and Phe 117 of the (−) side, and double Cys 190–191 and Tyr 195 of the (+) side. Cluster 2 comprises residues Asn 107 and Ala 108 of the (−) side, Tyr 195 of the (+) side, Phe 104, and Thr 143 of the (−) side, Trp 147 of the (+) side, and Val 109, Phe 117, and Leu 119 of the (−) side. The binding orientations of clusters 1 and 2 are shown in Figure 3. Compounds **1a** and **1b** and both enantiomers of **2** (**2a**

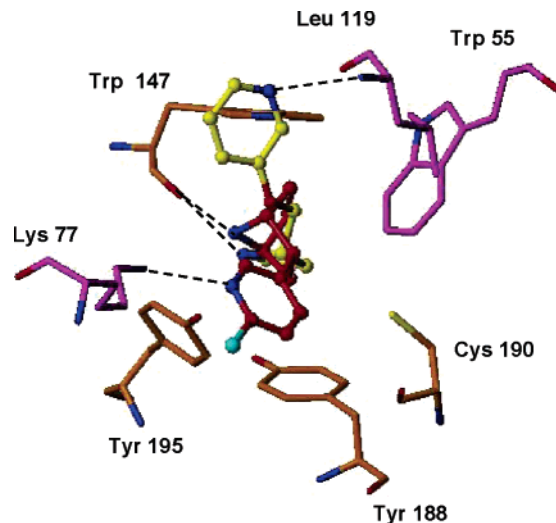


**Figure 3.** Ligand binding to the rat  $\alpha 4\beta 2$  model: docking of (−)-epibatidine (**1b**) as a representative of a toxic ligand (colored according to atom type, with the carbon atoms shown in red and the chlorine atom shown in cyan) and A-85380 (**4**) as a representative of a nontoxic ligand (colored according to atom type, with the carbon atoms shown in yellow) in clusters 1 and 2, respectively. Residues on the (+) and (−) sides are colored according to atom type, with the carbon atoms shown in orange and magenta, respectively. All residues and docked compounds are displayed as capped sticks and ball-and-stick figures, respectively. H-bonds as defined in Figure 2 are represented by black dashed lines.

and **2b**) docked in a similar orientation (cluster 1) as shown in Figure 3 for **1b**. On the other hand, compounds **3**, **4**, and **6** docked in another orientation (cluster 2), which is represented by **4** in Figure 3. The common features between the two clusters are (1) the orientation of the positively charged nitrogen, pointing toward the aromatic residues of the (+)-side Trp 147 (the homologue of Trp 143 in AChBP) and the Tyr 188, 195 and Trp 55 of the (−) side and (2) the H-bond between the NH of the positively charged nitrogen and the carbonyl of Trp 147 on the (+) side of the  $\alpha 4$  subunit. The former common feature suggests the importance of the cation– $\pi$  interactions between the ligand and the receptor binding site. The described orientation of **6** agrees with that found by Costa et al.<sup>23</sup> The pocket of aromatic residues, present in AChBP, is conserved by the homology in the binding domain of the nicotinic subunit. Residues Trp 147 and Tyr 188, 195 of the (+) side and Trp 55 of the (−) side are assumed to be involved in cation– $\pi$  interactions with the cationic center of the ligand.<sup>27</sup> As the homologue Trp 143 in AChBP, Trp 147 plays an important role for this type of interactions, which is confirmed by its central 3D orientation in the binding cavity. In both clusters, the carbonyl of the Trp 147 on the (+) side of the  $\alpha 4$  subunit makes an H-bond with the NH of the positively charged nitrogen of the compounds **1a**, **1b**, **2a**, **2b**, and **4**, further stabilizing the orientation of the ligands (Figure 3). This type of H-bond is also present with HEPES in the X-ray structure of AChBP (Figure 2), confirming the importance of this interaction. The ligands **1a**, **1b**, **2a**, **2b**, and **4**, which, of all the compounds of the chosen series, have the highest affinity for the rat  $\alpha 4\beta 2$  neuronal nicotinic subtype (Table 1), bind with the highest consensus score, in the orientation of either cluster 1 or cluster 2.

Although toxic and nontoxic ligands share the same cation- $\pi$  interactions with the protein, the rest of the molecule occupies a different moiety of the binding pocket. This different orientation is characterized by a distinct H-bond pattern. Cluster 1 is characterized by the H-bond between the pyridine nitrogen of the ligand and the nitrogen of the side chain of Lys 77 on the (-) side, whereas in cluster 2, the H-bond between the main chain amide of the Leu 119 on the (-) side and the pyridine nitrogen is depicted (Figure 3). In the case of **6**, an H-bond between the carbonyl oxygen and a molecule of water has been reported.<sup>23</sup> This suggests that the interaction between an H-bond acceptor atom of the ligand and an H-bond donor atom is important for affinity, whereas their location, in addition to stabilizing a certain receptor active conformation, seems to differentiate between ligands that are clinically toxic such as **1** and **2** and those that are clinically nontoxic such as **3**, **4**, and **6**. In our case, not considering a molecule of water in the binding of the ester moiety of **6** might be the reason for the low consensus score of 2 (Table 1).

The influence of the pyridine nitrogen in compound **5** shifting from the meta position to the ortho (**14**) and para (**15**) positions on binding orientation and binding affinity was investigated. The three ligands **5**, **14**, and **15** docked in the same orientation (cluster 3) with lower consensus scores than those found in clusters 1 and 2 (Table 1). Compound **5** showed a higher consensus score, which is in agreement with its higher binding affinity (Table 1). The positively charged nitrogen of the ligands was directed toward the aromatic pocket of the binding cavity but not as deeply as in clusters 1 and 2. The fact that ligands **5**, **14**, and **15** are further from the Trp 147 and Tyr 188, 195 on the (+) side and the Trp 55 on the (-) side decreases the number of favorable interactions with the binding site, lowering the consensus score relative to that found for clusters 1 and 2. The position of the nitrogen in the pyridine ring also seems to be critical for the affinity. The nitrogen of **5** does not make any relevant contacts, whereas the nitrogen of **15**, because of the increased vicinity, undergoes a repulsion from the carbonyl oxygen of Cys 190 on the (+) side of the  $\alpha 4$  subunit. This repulsive effect accounts for the 5 orders of magnitude difference in affinity between these two ligands, despite the presence of the stabilizing H-bond between the NH of the positively charged nitrogen and the oxygen carbonyl of Trp 147 on the (+) side of the  $\alpha 4$  subunit. Compound **14** loses the H-bond with Trp 147 compared to its meta and ortho derivatives, but its orientation is not influenced by the repulsive effect as is that of **15**. This is in agreement with the fact that the affinity of **14** is lower than that of **5** and higher than that of **15** (Table 1). Compound **10** docked in the same cluster 3 with the positively charged nitrogen pointing inside the binding cavity, but this time the aromatic oxazol-ring of the ligand facilitated the H-bond between the aromatic nitrogen and the side chain NH of Lys 77 on the (-) side of the  $\beta 2$  subunit, which is not present with **14** and **15**, thereby increasing its consensus score. This is in agreement with the values of the binding affinity constant which shows that **10** has affinity in the

nanomolar range as does **5** and has much higher affinity than **14** and **15** (Table 1).

The effect of the insertion of a second nitrogen in the pyridine ring of the ligand on the affinity was also studied. The docking of compounds **11** and **8**, which are both derivatives of **5**, gave the lowest consensus score of 0 (cluster 4). The orientation of the docked ligand **11** is different from that of docked compounds **4** and **5**. The positively charged nitrogen of the ligand points out of the tryptophan moiety of the binding cavity, losing the important cation- $\pi$  interactions. This orientation is stabilized by the hydrophobic interactions between residues of the binding site and the aromatic moiety of the molecule. This switching effect of these docked ligands is probably due to the repulsion between the nitrogens of the aromatic ring of the ligand and the carbonyl oxygen of Cys 190 on the receptor side, which would occur if the ligands would bind with the same orientation as compound **5**. As a consequence, the two ligands in the docked orientation lose the cation- $\pi$  interactions, lowering the consensus score and thus reflecting lower affinity compared to **5** (Table 1).

In the case of **8**, the low consensus score of 0 does not represent low affinity because although the ligand binds less than **5**, its affinity is still in the nanomolar range (Table 1). The scores obtained with **8** and **11** are in agreement with a previous report showing that the energy of the interaction of an H-bond donor with a pyridine nitrogen is less favorable when a second nitrogen is introduced into the aromatic ring, as in the case of diazine.<sup>28</sup> The same effect on the orientation, due to the presence of a second nitrogen, was also found with **12**, which docked in the same cluster 4 (Table 1).

The best docking orientation of ligands, which have an oxygen bridge between the pyridine and the aliphatic cycle moieties, was observed for **4** (cluster 2), in which the size of the aliphatic cycle is decreased. Large and hindered aliphatic cycles make it difficult for the ligand to enter deeply into the binding cavity, losing the possibility of establishing cation- $\pi$  interactions, which favor ligand binding to the receptor. This explains why decreasing the size of the aliphatic part of the ligand causes the binding affinity to increase.<sup>29</sup>

Enantiomers **1a**, **1b**, **2a**, and **2b** docked well in cluster 1, and they are toxic compounds. Ligands **3**, **4**, and **6**, which docked in cluster 2, are nontoxic compounds (Table 1). Compound **10**, which docked in cluster 3 (Table 1), establishes interactions similar to that of **1**. Despite this, the orientation of **10** is different and enters less deeply into the binding site cavity, as we find in cluster 4, causing loose cation- $\pi$  interactions. This may also explain the decreased binding affinity of **10**.

Regarding the  $\alpha 3\beta 4$  binding site, enantiomers **1a**, **1b**, **2a**, and **2b**, which are potent agonists toward the ganglionic  $\alpha 3\beta 4$  subtype,<sup>10,26</sup> docked well. Two clusters were identified. Clusters A and B are shown in Figure 4. In cluster A, the positively charged nitrogen of **1b** (Figure 4) points toward the aromatic pocket (Trp 147, 55 and Tyr 188, 195), again revealing the importance of cation- $\pi$  interactions between the ligand and the receptor binding site.<sup>27</sup> The absence of the H-bond interaction, between the side chain Lys 77 of the (-) side and the ligand pyridine nitrogen, present in the  $\alpha 4\beta 2$  binding cavity, is caused by the replacement of

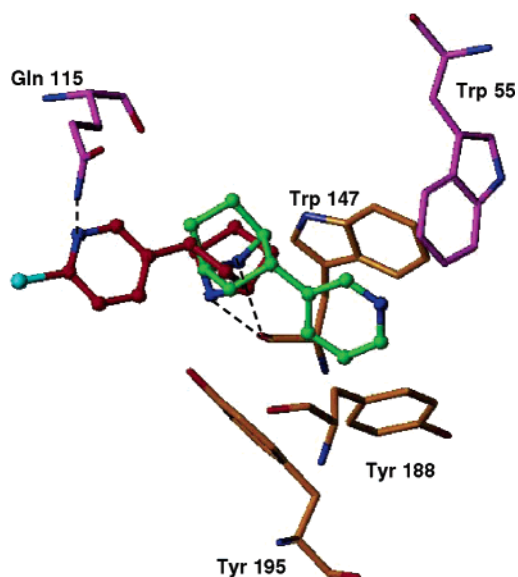


**Figure 4.** Ligand binding to the rat  $\alpha 3\beta 4$  model: docking of **1b** (colored according to atom type, with carbon atoms shown in red) and (+)-dechloroepibatidine (**2a**) (colored according to atom type, with carbon atoms shown in green) in clusters A and B, respectively. Residues on the (+) and (–) sides are colored according to atom type, with the carbon atoms shown in orange and magenta, respectively. All residues and docked compounds are displayed as capped sticks and ball-and-stick figures, respectively. H-bonds as defined in Figure 2 are represented by black dashed lines. For the sake of clarity, the point of view has been rotated compared to the rat  $\alpha 4\beta 2$  model (Figure 3).

the residue Lys with Ile. This is in agreement with the fact that compound **1** has a lower affinity toward the ganglionic subtype<sup>30</sup> than it has toward  $\alpha 4\beta 2$ . Moreover, the NH of the positively charged nitrogen of the enantiomers **1a**, **1b**, and **2b** forms an H-bond with the oxygen carbonyl of Trp 147 of the (+) side of the  $\alpha 3$  subunit. The nitrogen of the pyridine ring establishes an H-bond with the hydrogen of the side chain  $\text{NH}_2$  of Gln 115 of the (–) side. In cluster B, the NH of the positively charged nitrogen of **2a** (Figure 4) still forms an H-bond with the oxygen carbonyl of Trp 147, but the pyridine ring is stabilized by the hydrophobic interactions within the pocket formed by the aromatic residues (Trp 147, 55 and Tyr 188, 195) inside the binding cavity.

Compound **6** docked poorly into the binding cavity (Table 1), and this may be explained, as in the case of  $\alpha 4\beta 2$ , as the result of not considering the molecule of water involved in the H-bond with the carbonyl oxygen of **6** that was reported by Costa et al.<sup>23</sup>

Compounds **4** and **5** and their derivatives, which have a flexible ether moiety and do not show toxicity, did not dock into the binding cavity (Table 1). This confirms that the presence of an oxygen between the pyridine and the aliphatic moieties decreases the ligand affinity toward the ganglionic subtype with an increase of selectivity toward the neuronal subtype.

The docking into the  $\alpha 3\beta 4$  model of ligands, which contain constrained C–O–C or C–C–C– angles such as ligand **3** and ligands **9** and **13** (Figure 1), was performed.

All three molecules docked well into the cavity as did **2a** (cluster B). In fact, the positively charged nitrogen in all cases pointed away from the aromatic surrounding

of the (+) side of the  $\alpha$  subunit, this time making an H-bond interaction with the oxygen of the carbonyl of the residue Gln 115 of the (–) side of the  $\beta$  subunit. The aromatic nitrogen of ligand **9** does not seem to play such an important role in the binding orientation to this ganglionic nAChR subtype. Despite the controversial activity of **9** on  $\alpha 3\beta x$  receptors (it shows activation in rat striatum but not in IMR32 cells) [unpublished data], these results suggest that introducing sterically constrained and planar C–O–C and C–C–C angles, as in ligands **3** and **9**, improves the docking of the ligand into the binding cavity in correspondence with an increase of the affinity to  $\alpha 3\beta 4$  receptor subtype, whereas flexibility abolishes it.

Compound **3**, which docks well into the  $\alpha 3\beta 4$  cavity, was proven to be clinically nontoxic by toxicity studies on mice performed in our group. [Westera, G., unpublished observation] Moreover, **3** was proven to behave as an agonist toward the ganglionic  $\alpha 3\beta 4$  subtype but with less potency than that of **1** and **2**. [ref 26; Bertrand, D., personal communication] This might explain why, even if **3** binds to the ganglionic nAChR subtype, because of unfavorable binding kinetics, it does not cause the peripheral side effects that occur with compounds **1** and **2**.

## Conclusions

A molecular docking study was performed on the binding site of the geometrically and stereochemically refined rat neuronal  $\alpha 4\beta 2$  and ganglionic  $\alpha 3\beta 4$  nicotinic subtype receptors at the interface between the  $\alpha$  and the  $\beta$  subunits.

The chosen nAChR ligands **1**–**15** bind with binding affinities ranging from micromolar to picomolar and include necessary pharmacophores in their structure (e.g., a positively charged nitrogen; an electron-donor atom, such as the pyridine nitrogen, which is capable of H-bonding; and a hydrophobic area generally formed by aliphatic cycles). The docking results and the consensus scores of the docked molecules reveal the putative binding modes of the ligands and suggest a structure–activity relationship. The consensus score evaluation of the docking and thus their ranking on the  $\alpha 4\beta 2$  model showed significant correlation with the differences in binding affinities, whereas single-scoring functions did not allow any discrimination. The investigation of the selectivity of the ligands between central neuronal and peripheral ganglionic nicotinic subtypes showed interesting trends. Of all the examined ligands, both enantiomers of **1** and **2** docked with high consensus scores in both binding cavities (i.e.,  $\alpha 4\beta 2$  and  $\alpha 3\beta 4$ ). This is in agreement with their peripheral side effects, which are linked to  $\alpha 3\beta 4$  agonism, observed during their clinical use. Two important clusters of docking (**1** and **2**) are found in the  $\alpha 4\beta 2$  model, involving ligands such as **1**, **2**, **3**, **4**, and **6**. The orientation of the docked molecules underline the importance of cation– $\pi$  interactions between the positively charged nitrogen of the ligand and the aromatic side chains of the residues Trp 147 and Tyr 188, 195 on the (+) side and Trp 55 on the (–) side and of the H-bond contacts between the pyridine nitrogen or oxygen carbonyl of the ligand and the backbone NH of the residues mainly on the (–) side of the complementary  $\beta 2$  subunit. The ligands that docked

in clusters 1 and 2 were the clinically toxic compounds **1** and **2** and the clinically nontoxic compounds **3**, **4**, and **6**, respectively. Thus, for the design of nAChR ligands lacking toxicity, compounds should fill the moiety of the pocket surrounding cluster 2 orientation. Regarding the docking of the ligands into the  $\alpha 3\beta 4$  model binding site, which seems to be highly correlated with the agonistic potency of the ligands, the results revealed two important factors. The presence of the oxygen atom between the pyridine ring and the aliphatic moiety plays an important role in abolishing affinity to the ganglionic receptor, represented by the impossibility of finding a binding orientation within the binding site. Indeed, its presence increases the subtype selectivity toward the neuronal receptor by reducing the affinity toward peripheral nicotinic subtypes and thus decreasing the toxicity of the ligands. If the flexibility around the C–O–C or C–C–C– angles is constrained, as with ligands **3** and **9**, the ability to bind into the  $\alpha 3\beta 4$  binding cavity might increase. As a consequence, the tridimensional structure of **1** seems to be a good template for ligands with high affinity toward the ganglionic receptor but low subtype selectivity.

In general, the consensus score rankings of the docked molecules showed a relationship with the inhibition constant ( $K_i$ ) values taken from the literature (see Table 1).

The results obtained from the docking investigations showed that the models are useful to design subtype-specific compounds with high affinity toward the neuronal  $\alpha 4\beta 2$  subtype (preferably binding in the cluster 2 mode) and with enough flexibility to prevent them from binding to the ganglionic  $\alpha 3\beta 4$  subtype. The design of such compounds would improve their safety in therapeutic and diagnostic use and enable clinical application in neurological diseases.

## Experimental Section

**Toxicity Studies of Compound ( $\pm$ )-2.** An acute intravenous toxicity study of the racemic *N*-methyl-dechloropibatidine in rats and mice was performed by the Research and Consulting Company Ltd. (RCC), Itingen, Switzerland. The study should provide a rational basis for risk assessment in man. The study was performed in mice [HanIbm: NMRI (SPF)]. Nine animals (6 male and 3 female) were treated with 1.2, 0.12, or 0.012  $\mu\text{mol/kg}$  of *N*-methyl-dechloropibatidine. The test substance was injected intravenously into the caudal vein.

The median lethal dose (LD50) of compound ( $\pm$ )-2 after a single intravenous injection in mice and rats of both sexes, observed over a period of 15 days, was thus established to be between 0.012 and 1.12  $\mu\text{mol/kg}$  body weight; no animals died at 0.012  $\mu\text{mol/kg}$ , but all animals treated with 1.2  $\mu\text{mol/kg}$  or 0.12  $\mu\text{mol/kg}$  died spontaneously within 10 min after treatment.

## References

- Galzi, J.-L.; Changeux, J. P. Neurotransmitter-gated ion channels as unconventional allosteric proteins. *Curr. Opin. Struct. Biol.* **1994**, *4*, 554–565.
- Le Novère, N.; Changeux, J. P. Molecular evolution of the nicotinic acetylcholine receptor: an example of multigene family in excitable cells. *J. Mol. Evol.* **1995**, *40*, 155–172.
- Léna, C.; Changeux, J. P.; Mulle, C. Evidence for “preterminal” nicotinic receptors on GABAergic axons in the rat interpeduncular nucleus. *J. Neurosci.* **1993**, *13*, 2680–2688.
- Changeux, J. P.; Edelstein, S. J. Allosteric receptors after 30 years. *Neuron* **1998**, *21*, 959–980.
- Holladay, M. W.; Dart, M. J.; Lynch, J. K. Neuronal nicotinic acetylcholine receptors as targets for drug discovery. *J. Med. Chem.* **1997**, *40*, 4169–4194.
- Badio, B.; Daly, J. W. Epibatidine, a potent analgetic and nicotinic agonist. *Mol. Pharmacol.* **1994**, *45*, 563–569.
- Abreo, M. A.; Lin, N.-H.; Garvey, D. S.; Gunn, D. E.; Hettinger, A.-M.; et al. Novel 3-pyridyl ethers with subnanomolar affinity for central neuronal nicotinic acetylcholine receptors. *J. Med. Chem.* **1996**, *39*, 817–825.
- Holladay, M. W.; Wasicak, J. T.; Lin, N. H.; He, Y.; Ryther, K. B.; et al. Identification and initial structure–activity relationships of (R)-5-(2-azetidylmethoxy)-2-chloropyridine (ABT-594), a potent, orally active, nonopioid analgesic agent acting via neuronal nicotinic acetylcholine receptors. *J. Med. Chem.* **1998**, *41*, 407–412.
- Lloyd, G. K.; Williams, M. Neuronal nicotinic acetylcholine receptors as novel drug targets. *J. Pharmacol. Exp. Ther.* **2000**, *292*, 461–467.
- Gerzanich, V.; Peng, X.; Wang, F.; Wells, G.; Anand, R.; et al. Comparative pharmacology of epibatidine: a potent agonist for neuronal nicotinic acetylcholine receptors. *Mol. Pharmacol.* **1995**, *48*, 774–782.
- Lembeck, F. Epibatidine: high potency and broad spectrum activity on neuronal and neuromuscular nicotinic acetylcholine receptors. *Naunyn-Schmiedeberg Arch. Pharmacol.* **1999**, *359*, 378–385.
- Brejč, K.; Van Dijk, W. J.; Klaassen, R. V.; Schuurmans, M.; van der Oost, J.; et al. Crystal structure of an ACh-binding protein reveals the ligand-binding domain of nicotinic receptors. *Nature* **2001**, *411*, 269–276.
- Smit, A. B.; Syed, N. I.; Schaap, D.; Van Minnen, J.; Klumpermann, J.; et al. A glia-derived acetylcholine-binding protein that modulates synaptic transmission. *Nature* **2001**, *411*, 261–268.
- Cornell, W. D.; Cieplak, P.; Bayly, C. I.; Gould, I. R.; Merz, K. M.; et al. A second-generation force field for the simulation of proteins, nucleic acids, and organic molecules. *J. Am. Chem. Soc.* **1995**, *117*, 5179–5197.
- Laskowski, R. A.; MacArthur, M. W.; Moss, D. S.; Thornton, J. M. PROCHECK: a program to check the stereochemical quality of protein structures. *J. Appl. Crystall.* **1993**, *26*, 283–291.
- Dart, M. J.; Wasicak, J. T.; Ryther, K. B.; Schrimpf, M. R.; Kim, K. H.; et al. Structural aspects of high affinity ligands for the alpha 4 beta 2 neuronal nicotinic receptor. *Pharm. Acta Helv.* **2000**, *74*, 115–123.
- Lin, N. H.; Abreo, M. A.; Gunn, D. E.; Lebold, S. A.; Lee, E. L.; et al. Structure–activity studies on a novel series of cholinergic channel activators based on a heteroaryl ether framework. *Bioorg. Med. Chem. Lett.* **1999**, *9*, 2747–2752.
- Rarey, M.; Kramer, B.; Lengauer, T. Multiple automatic base selection: protein–ligand docking based on incremental construction without manual intervention. *J. Comput.-Aided Mol. Des.* **1997**, *11*, 369–384.
- Kramer, B. R., M.; Lengauer, T. Evaluation of the FLEXX incremental construction algorithm for protein–ligand docking. *Proteins: Struct., Funct., Genet.* **1999**, *37*, 228–241.
- Triplos Home Page. <http://www.triplos.com/sciTech/inSilicoDisc/virtualScreening/cscore.html> (accessed May 2005).
- Bissantz, C.; Folkers, G.; Rognan, D. Protein-based virtual screening of chemical databases. 1. Evaluation of different docking/scoring combinations. *J. Med. Chem.* **2000**, *43*, 4759–4767.
- Le Novère, N.; Grutter, T.; Changeux, J. P. Models of the extracellular domain of the nicotinic receptors and of agonist- and  $\text{Ca}^{2+}$ -binding sites. *Proc. Natl. Acad. Sci. U.S.A.* **2002**, *99*, 3210–3215.
- Costa, V.; Nistri, A.; Cavalli, A.; Carloni, P. A structural model of agonist binding to the  $\alpha 3\beta 4$  neuronal nicotinic receptor. *Br. J. Pharmacol.* **2003**, *140*, 921–931.
- Celie, P. H. N.; van Rossum-Fikkert, S. E.; van Dijk, W. J.; Brejč, K.; Smit, A. B.; Sixma, T. K. Nicotine and carbamylcholine binding to nicotinic acetylcholine receptors as studied in AChBP crystal structures. *Neuron* **2004**, *41*, 907–914.
- Beene, D. L.; Brandt, G. S.; Zhong, W.; Zacharias, N. M.; Lester, H. A.; et al. Cation–pi interactions in ligand recognition by serotonergic (5-HT3A) and nicotinic acetylcholine receptors: the anomalous binding properties of nicotine. *Biochemistry* **2002**, *41*, 10262–10269.
- Spang, J. E.; Bertrand, S.; Westera, G.; Patt, J. T.; Schubiger, P. A.; et al. Chemical modification of epibatidine causes a switch from agonist to antagonist and modifies its selectivity for neuronal nicotinic acetylcholine receptors. *Chem. Biol.* **2000**, *7*, 545–555.
- Zhong, W.; Gallivan, J. P.; Zhang, Y.; Li, L.; Lester, H. A.; et al. From ab initio quantum mechanics to molecular neurobiology: a cation–pi binding site in the nicotinic receptor. *Proc. Natl. Acad. Sci. U.S.A.* **1998**, *95*, 12088–12093.
- Nobeli, I.; Price, S. L.; Lommerse, J. P. M.; Taylor, R. Hydrogen bonding properties of oxygen and nitrogen acceptors in aromatic heterocycles. *J. Comput. Chem.* **1997**, *18*, 2060–2074.



- (29) Nielsen, S. F.; Nielsen, E. O.; Olsen, G. M.; Liljefors, T.; Peters, D. Novel potent ligands for the central nicotinic acetylcholine receptor: synthesis, receptor binding, and 3D-QSAR analysis. *J. Med. Chem.* **2000**, *43*, 2217–2226.
- (30) Sihver, W.; Nordberg, A.; Långström, B.; Mukhin, A. G.; Koren, A. O.; et al. Development of ligands for in vivo imaging of cerebral nicotinic receptor. *Behav. Brain Res.* **2000**, *113*, 143–157.
- (31) Sullivan, J. P.; Decker, M. W.; Brioni, J. D.; Donnelly Roberts, D.; Anderson, D. J.; et al. ( $\pm$ )-Epibatidine elicits a diversity of in vitro and in vivo effects mediated by nicotinic acetylcholine receptors. *J. Pharmacol. Exp. Ther.* **1994**, *271*, 624–631.
- (32) Sharples, C. G. V.; Wonnacott, S. Biotrend Home Page. <http://www.biotrend.com/pdf/nicotinicrev.pdf> (accessed Aug 2004).
- (33) Xiao, Y.; Meyer, E. L.; Thompson, J. M.; Surin, A.; Wroblewski, J.; Kellar, K. J. Rat  $\alpha 3\beta 4$  subtype of neuronal nicotinic acetylcholine receptor stably expressed in a transfected cell line: pharmacology of ligand binding and function. *Mol. Pharmacol.* **1998**, *54*, 322–333.
- (34) Sihver, W.; Langstrom, B.; Nordberg, A. Ligands for in vivo imaging of nicotinic receptor subtypes in Alzheimer brain. *Acta Neurol. Scand.* **2000**, *176*, 27–33.
- (35) Schwartz, R. D.; McGee, R., Jr.; Kellar, K. J. Nicotinic cholinergic receptors labeled by [ $^3$ H]acetylcholine in rat brain. *Mol. Pharmacol.* **1982**, *22*, 56–62.
- (36) J. T. Baker Home Page. <http://www.jtbaker.com/msds/englishhtml/a0830.htm> (accessed Aug 2004).
- (37) Decker, M. W.; Brioni, J. D.; Sullivan, J. P.; Buckley, M. J.; Radek, R. J.; et al. (S)-3-Methyl-5-(1-methyl-2-pyrrolidinyl)-isoxazole (ABT 418): a novel cholinergic ligand with cognition-enhancing and anxiolytic activities: II. in vivo characterization. *J. Pharmacol. Exp. Ther.* **1994**, *270*, 319–328.

JM040881A